

# Corrosion Inhibition Behavior of 9-Hydroxyrisperidone as a Green Corrosion Inhibitor for Mild Steel in Hydrochloric Acid: Electrochemical, DFT and MD Simulations Studies

H. Lgaz<sup>1,2</sup>, R. Salghi<sup>1,\*</sup>, Ismat H. Ali<sup>3,\*</sup>

<sup>1</sup> Laboratory of separation processes, Faculty of Science, University Ibn Tofail PO Box 242. Kenitra, Morocco.

<sup>2</sup>Laboratory of Applied Chemistry and Environment, ENSA, University Ibn Zohr, PO Box 1136. Agadir, Morocco.

<sup>3</sup>Department of Chemistry, College of Science, King Khalid University, P. O. Boox, Postal Code 61413, Saudi Arabia

\*E-mail: [ismathassanali@gmail.com](mailto:ismathassanali@gmail.com); [r.salghi@uiz.ac.ma](mailto:r.salghi@uiz.ac.ma);

Received: 22 August 2017 / Accepted: 27 October 2017 / Online Published: 1 December 2017

---

A green corrosion inhibitor namely, 9-Hydroxyrisperidone (HRD) was investigated for their influence on mild steel corrosion in 1 M HCl using weight loss, Tafel polarization, electrochemical impedance spectroscopy (EIS) and surface morphology techniques. Quantum chemical calculations were also conducted to corroborate experimental findings. The tested compound is mixed type inhibitor following Langmuir adsorption isotherm and involved competitive physisorption and chemisorption mechanisms. The results from electrochemical impedance spectroscopy tests reveal an increase in polarization resistance. Scanning Electron Microscopy (SEM) analyses of steel surfaces in acid-inhibitor solutions showed that tested compound protects mild steel surface effectively. The inhibition property was further elucidated by theoretical approaches; quantum chemical calculation and Molecular Dynamic (MD) simulation.

---

**Keywords:** Inhibition, Corrosion, 9-Hydroxyrisperidone, Steel, DFT, Molecular Dynamic.

## 1. INTRODUCTION

The study of corrosion is of paramount importance because of the direct and indirect losses caused by this scourge. At the economic level, more than a quarter of the world's steel production is degraded due to a corrosion problem[1]. Acid solutions, on the other hand, are widely used in acid cleaning, stimulation of oil wells, and the elimination of localized deposits (tartar not uniformly spread, rust, bacterial deposits, etc.). The aggressiveness of these acid solutions leads to the use of

corrosion inhibitors which are indispensable in order to limit the attack of metallic materials. Of the commercially available acids, hydrochloric acid is the most frequently used and is increasingly replacing sulfuric acid[2,3]. The economic and environmental components are nevertheless underlying in the fight against corrosion and will be approached to raise awareness of the principles of economic management and respect for environmental constraints. The use of corrosion inhibitors as a means of protection is necessary in many industrial cases: surface preparation, transport and storage of metals, cooling circuits, rehabilitation of reinforced concrete, painting and cathodic protection[4–6]. The adsorption characteristics mild steel of corrosion inhibitors depend upon the chemical moiety of the molecule, type of functional groups and the electron density at the donor atoms. Organic compounds, containing heteroatom's (N, O, S, and P), electronegative functional groups,  $\pi$ - electrons and aromatic rings as electron density rich centers which are considered as good adsorptive centers[7–9]. These heterocyclic organic inhibitors get adsorb onto the steel surface or form protective insoluble layer and block corrosion sites, which reduces contact of corroding material with the corrosive medium/steel[10]. The current trend is towards green or friendly inhibitors of the environment[11–15]. These inhibitors must be non-toxic and capable of ensuring good protection of metals and alloys.

In this paper, inhibitory effect of 9-Hydroxyrisperidone (HRD) on the mild steel corrosion in hydrochloric acid solution (1M HCl) was studied using chemical, electrochemical (PDP and electrochemical impedance spectroscopy), DFT and MD simulations studies. The mild steel morphologies were evaluated with the aid of SEM.

## 2. EXPERIMENTAL

### 2.1. Materials and inhibitor

Mild Steel with the following chemical composition 0.370 % C, 0.230 % Si, 0.680 % Mn, 0.016 % S, 0.077 % Cr, 0.011 % Ti, 0.059 % Ni, 0.009 % Co, 0.160 % Cu and balance Fe, was used for all the experiments. The surface of mild steel was abraded and polished mechanically with 360 to 1600 grade of emery paper (SiC). The working electrode was thereafter degreased with acetone, rinsed with bidistilled water and then dried at room temperature before further use. The aggressive medium (1 M HCl) was prepared by diluting a reagent of analytical grade HCl 37% (from Sigma-Aldrich) with double-distilled water. The 9-Hydroxyrisperidone was purchased from Sigma-Aldrich. The chemical structure of tested compound is represented below:

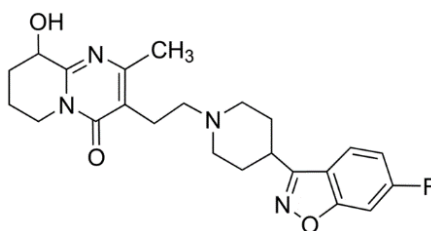


**Figure 1.** Molecular structure of 9-Hydroxyrisperidone.

## 2.2. Weight loss tests and electrochemical measurements

The samples of mild steel used in the gravimetric method are in the form of a square of ( $1.8 \times 1.8 \times 0.06 \text{ cm}^3$ ) dimension were polished with 360 to 1600 grits of emery paper and suspended for 6 hours of immersion time with different concentrations of 9-Hydroxyrisperidone (HRD), in absence of agitation maintained at a constant temperature (303 K). At the end of the experiment, the sample is removed from the solution and then cleaned with distilled water. At the end, the corrosion products will be removed by chemical etching in 7M nitric acid solution for 15 s and the samples will be weighed again.

Three-electrode electrochemical glass cell consisting of a platinum (as counter electrode, CE), a saturated calomel KCl electrode (ECS) (as reference electrode, RE), and mild steel (as working electrode, WE) with freshly pre-treated reactive surface area of  $1 \text{ cm}^2$  was used for electrochemical studies. The WE was left to undergo free corrosion in the test solution for 30 min, within which a stable open circuit potential (OCP) was reached, and after which electrochemical perturbation was applied. For the Tafel polarization measurements, the potentials were swept between -800 mV to -200 mV at the scan rate of 1 mV/s relative to the corrosion potential ( $E_{\text{corr}}$ ). For the EIS measurements, AC current signal was passed through the system within the frequency range of 10 mHz to 100 KHz at 10 mV amplitude.

## 2.2. DFT and Molecular dynamic simulations

The quantum-based calculations were conducted using Materials Studio software package (version 6.0) at DFT/GGA level using BOP functional and DNP basis set on all atoms[16–18]. The calculations started without any geometry constraints until full geometry optimizations. The COSMO[19] controls were used for solvation effects (aqueous phase). The ionization energy and the electronic affinity were determined by the values of the energies of the HOMO and LUMO orbital[20]:

$$I = -E_{\text{HOMO}} \quad (1)$$

$$A = -E_{\text{LUMO}} \quad (2)$$

The values of I and A are exploited in order to find the values of the electronegativity and the global hardness of the inhibitory molecule[21]:

$$\chi = \frac{I+A}{2} \quad (3)$$

$$\eta = \frac{I-A}{2} \quad (4)$$

The fraction of electrons transferred ( $\Delta N$ ) from inhibitor to metallic surface was calculated using the equation[22]:

$$\Delta N = \frac{\phi - \chi_{\text{inh}}}{2(\eta_{\text{Fe}} + \eta_{\text{inh}})} \quad (5)$$

Where  $\phi$  is the work function used as the appropriate measure of electronegativity of iron, and  $\eta_{\text{Fe}} = 0$ . The value of  $\phi = 4.82 \text{ eV}$  for Fe (110) surface which is reported to have higher stabilization energy[23–26]. The local reactivity of inhibitor molecules (nucleophilic and electrophilic attacks) were obtained by condensed Fukui functions[27] using the following equations[28]:

$$f_k^+ = q_k(N+1) - q_k(N) \quad (6)$$

$$f_k^- = q_k(N) - q_k(N-1) \quad (7)$$

where  $q_k(N-1)$ ,  $q_k(N+1)$ ,  $q_k(N)$  are the charges of the cationic, anionic and neutral molecule, respectively.

In all molecular modeling and simulation procedures, molecular dynamics (MD) simulation were carried out using Materials studio package[29] in a 10 x 10 super cell using the COMPASS force field with a time step of 1 fs and simulation time of 500 ps[29] in a simulation box of (24.82×24.82×35.69 Å<sup>3</sup>). The Temperature was fixed at 303 K. The binding and interactions energies are estimated by using following Equations[30]:

$$E_{\text{interaction}} = E_{\text{total}} - (E_{\text{surface+solution}} + E_{\text{inhibitor}}) \quad (8) \text{ and } E_{\text{Binding}} = -E_{\text{interaction}} \quad (9)$$

Where  $E_{\text{total}}$  is the total energy of the entire system  $E_{\text{surface+solution}}$  referred to the total energy of Fe (110) surface and solution without the inhibitor and  $E_{\text{inhibitor}}$  represent the total energy of inhibitor.

### 2.3. Surface characterization

The surface characteristics of mild steel specimens after immersing in aggressive solution for 6 h without and with 5×10<sup>-3</sup> M of inhibitor were examined using scanning electron microscopy (SEM (Hitachi TM-1000) ).

## 3. RESULTS AND DISCUSSION

### 3.1. Weight loss tests

The results in Table 1 shows the corrosion rate (W) and inhibition efficiency ( $\eta$  %) calculated by using the mass loss method at 303K. The ( $\eta$ ) values of the 9-Hydroxyrisperidone (HRD) are calculated using equation (10) and (11) and shown in Table 1.

$$W = \frac{m_0 - m}{St} \quad (10)$$

$$\eta_w (\%) = \frac{W_0 - W}{W_0} \times 100 \quad (11)$$

where  $m_0$  and  $m$  are the weight losses of mild steel without and with the inhibitor respectively,  $S$  is the total surface area,  $t$  is the immersion time,  $W_0$  and  $W$  are corrosion rates of mild steel samples in absence and presence of 9-Hydroxyrisperidone, respectively.

From this study, it can be observed that the corrosion rate decreased when the inhibitor concentration increased. This phenomenon is attributed to inhibitor's molecule which adsorbed at higher level of adsorption on the mild steel surface. It was also seen that the inhibition efficiency

increased with the increasing of the concentration of inhibitor. A stable inhibitor-film is formed on steel/solution interface. Besides, HRD suppresses effectively the metal dissolution, indicating a good inhibition performance of 9-Hydroxyrisperidone in 1 M HCl solution[31,32].

**Table 1.** Mild steel weight loss data and inhibition efficiency of 9-Hydroxyrisperidone at 303 K.

| Acid solution/Inhibitor | $W$ (mg cm <sup>-2</sup> h <sup>-1</sup> ) | $\eta_w$ (%) |
|-------------------------|--|--------------|
| 1 M HCl                 | 1.135                                      | ---          |
| 5×10 <sup>-3</sup>      | 0.068                                      | 94           |
| 1×10 <sup>-3</sup>      | 0.124                                      | 89           |
| 5×10 <sup>-4</sup>      | 0.192                                      | 83           |
| 1×10 <sup>-4</sup>      | 0.249                                      | 78           |

3.2. Tafel polarization curves

Tafel curves were recorded for mild steel in the blank (1 M HCl) and in the presence of 9-Hydroxyrisperidone at different concentrations and the plots are presented in Figure 2. Electrochemical parameters related to kinetics of the corrosion process were derived from extrapolation of the linear Tafel regions to the corrosion potential and the results are listed in Table 2. The potentiodynamic polarization inhibition efficiency (%) was then calculated from following equation:

$$\eta_{PDP} (\%) = \left[ 1 - \frac{i_{corr}}{i_{corr}^{\circ}} \right] \times 100 \tag{12}$$

where  $i_{corr}$  and  $i_{corr}^{\circ}$  are the corrosion current densities under uninhibited and inhibited conditions, respectively.

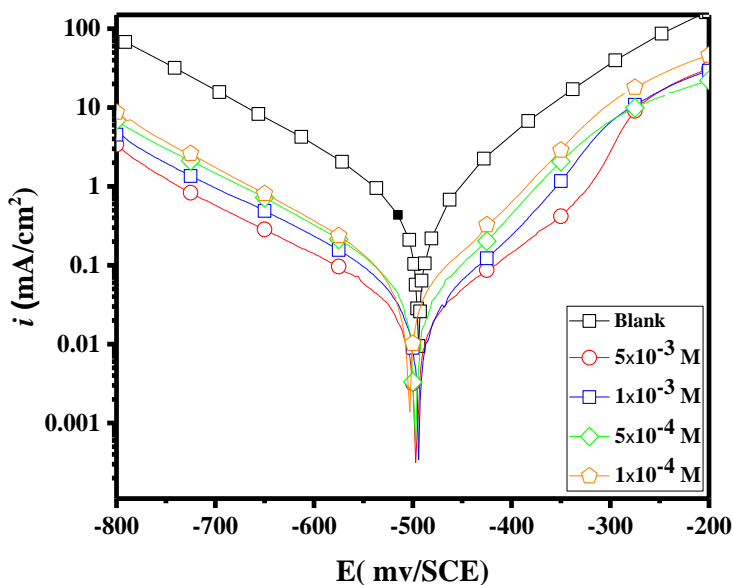


**Figure 2.** The PDP curves of mild steel in 1 M HCl and with 9-Hydroxyrisperidone at 303 K.

As can be understood from polarization curves, the addition of tested inhibitor to test solution causes no change in the identity of PDP curves, but become wider and extrapolated at lower current density, indicating that the inhibitor molecules interfere with reactive sites on metal electrode surface[7]. The PDP parameters listed in Table 2 indicate that increasing the concentration of inhibitor is accompanied with a decrease in  $i_{corr}$  since the ability of inhibitor molecules is enhanced to block more reactive sites that are necessary for corrosion reactions[33,34]. The features of the Tafel curves for the blank and inhibitor containing systems are akin, suggesting that 9-Hydroxyrisperidone retards corrosion by adsorbing on the steel surface without changing the corrosion mechanism[7]. Also judging from the shift in  $E_{corr}$  in Figure 2 and Table 2, 9-Hydroxyrisperidone can be inferred to be a mixed type inhibitor[35–37]. In other words, 9-Hydroxyrisperidone retards both the oxidative dissolution mild steel and reductive evolution of hydrogen gas.

**Table 2.** The PDP parameters and inhibition efficiency of mild steel at different contents of 9-Hydroxyrisperidone in 1 M HCl at 303K.

| Inhibitor | Concentration (M)  | $-E_{corr}$ (mV/SCE) | $-\beta_c$ (mV/dec) | $\beta_a$ (mV/dec) | $i_{corr}$ ( $\mu\text{A}/\text{cm}^2$ ) | $\eta_{PDP}$ (%) |
|-----------|--------------------|----------------------|---------------------|--------------------|--|------------------|
| Blank     | 1.0                | 496.0                | 162.0               | 132.2              | 564.0                                    | -                |
|           | $5 \times 10^{-3}$ | 499.3                | 153.11              | 134.7              | 32.9                                     | 94               |
|           | $1 \times 10^{-3}$ | 496.1                | 152.5               | 92.0               | 50.7                                     | 91               |
| HRD       | $5 \times 10^{-4}$ | 499.5                | 151.9               | 95.6               | 62.7                                     | 88               |
|           | $1 \times 10^{-4}$ | 506.2                | 149.6               | 94.8               | 81.7                                     | 85               |

3.3. Electrochemical impedance spectroscopy measurements

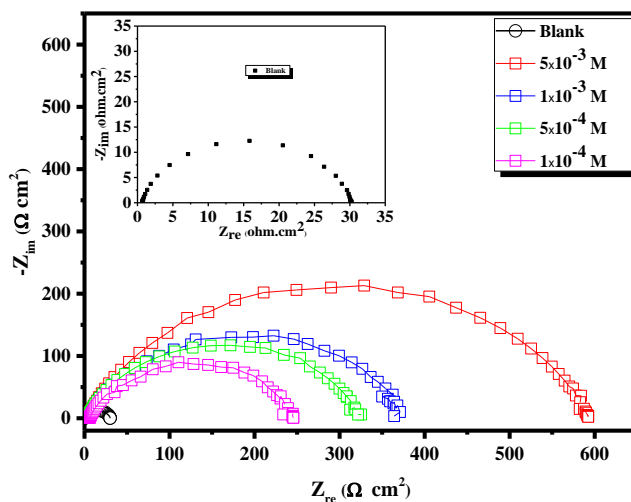


**Figure 2.** The EIS diagrams for mild steel with and without 9-Hydroxyrisperidone concentrations at 303 K.

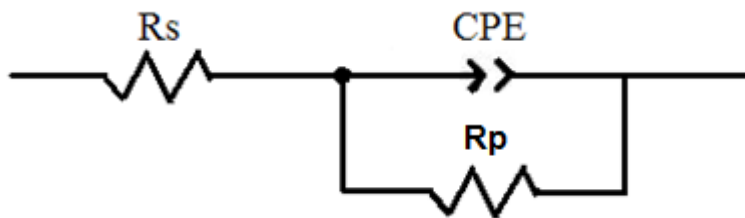


**Figure 3.** Equivalent electrical circuit.

The impedance spectroscopic data and corresponding Nyquist plots are represented in Table 3 and Fig. 3, respectively. The appearance of Nyquist plots both in the presence and absence of 9-Hydroxyrisperidone showed a single capacitive semicircle which indicate that the mechanism of corrosion process remains unchanged in the presence of inhibitor[8]. The diameter of capacitive loop increased with increase in 9-Hydroxyrisperidone concentration, which indicates the improved inhibition efficiency of this molecule at higher inhibitor concentrations.

The Nyquist diagrams were analyzed by fitting experimental Nyquist data to the simple equivalent circuit in Figure 3 which comprises the constant phase element (CPE), solution resistance (Rs) and polarization resistance (Rp). The impedance of CPE ( $Z_{CPE}$ ) represented by following equation[10]:

$$Z_{CPE} = \frac{1}{Y_0 (j\omega)^n} \tag{13}$$

Where:  $Y_0$  is the CPE coefficient,  $n$  the CPE exponent (phase shift),  $\omega$  the angular frequency and  $j$  stands for the imaginary unit. The interfacial capacitance  $C_{dl}$  can be calculated using the expression[38]:

$$C_{dl} = \sqrt[n]{Q \times R_p^{1-n}}$$

Inhibition efficiencies ( $\eta$  %) were calculated using the following equation[39]:

$$\eta_{EIS} (\%) = \left[ \frac{R_{p(inh)} - R_p}{R_{p(inh)}} \right] \times 100 \tag{14}$$

where,  $R_{p(inh)}$  and  $R_p$  are polarization resistances obtained in the presence and absence of 9-Hydroxyrisperidone, respectively.

**Table 3.** Nyquist parameters for mild steel in 1M HCl and with 9-Hydroxyrisperidone at 303 K.

| Inhibitor  | Concentration (M) | $R_{ct}$ ( $\Omega \times \text{cm}^2$ ) | $n$  | $Q \times 10^{-4}$ ( $\text{s}^n / \Omega \times \text{cm}^2$ ) | $C_{dl}$ ( $\mu\text{F}/\text{cm}^2$ ) | $\eta_{EIS}$ (%) |
|------------|-------------------|--|------|---|--|------------------|
| Blank      | 1.0               | 29.35                                    | 0.89 | 1.761   | 91.8633                                | -                |
| <b>HRD</b> | $5.10^{-3}$       | 589.8                                    | 0.78 | 0.3278  | 10.7711                                | 95               |
|            | $10^{-3}$         | 374.2                                    | 0.77 | 0.4135  | 11.9042                                | 92               |
|            | $5.10^{-4}$       | 320.1                                    | 0.80 | 0.4134  | 14.0212                                | 90               |
|            | $10^{-4}$         | 240.1                                    | 0.79 | 0.5934  | 19.1677                                | 87               |

As observed in Table 3, the values of  $n$  show deviation from unity which is attributed to deviation from ideal capacitive behavior due to inhomogeneity on metal surface[38,40]. As shown in Table 3, the value of  $C_{dl}$  decreases with increasing the inhibitor concentration, indicating the increase in the thickness of the electric double layer on the metal/solution interface and/or decrease in the value of dielectric constant due to the displacement of pre-adsorbed water molecules by the inhibitor[38,40]. The  $R_p$  values in the presence of 9-Hydroxyrisperidone increase upon further increase in concentration. This suggests that 9-Hydroxyrisperidone impede charge transfer corrosion process at higher concentrations.

### 3.4. Adsorption isotherm

From the above results, we can conclude that the coverage ratio of the surface  $\theta$  (IE% / 100), calculated using the weight loss and electrochemical measurements increases considerably with 9-Hydroxyrisperidone concentration indicating the more adsorption of 9-Hydroxyrisperidone on the surface of the steel[5,6]. The inhibition action of tested green molecule on metal surface depends on the extent of adsorption and nature of interaction with metal surface and which could be better understood by adsorption isotherm[10]. Various adsorption isotherms were fitted and best fit was obtained for Langmuir adsorption isotherm. According to Langmuir adsorption isotherm, the surface coverage ( $\Theta$ ) is related to inhibitor concentration ( $C_{inh}$ ) as[32]:

$$\frac{C_{inh}}{\theta} = \frac{1}{K_{ads}} + C_{inh} \quad (15)$$

where  $C_{inh}$  is the Concentration of 9-Hydroxyrisperidone and  $K_{ads}$  is the adsorption equilibrium constant of the adsorption process.

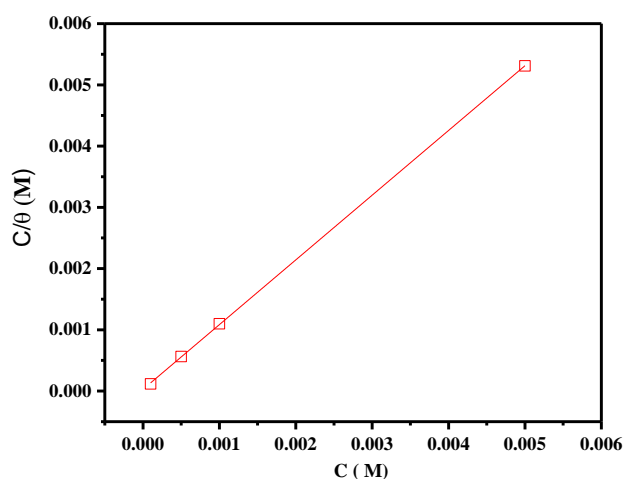


**Figure 5.** Langmuir isotherm plot of 9-Hydroxyrisperidone adsorbed on mild steel electrode in 1 M HCl.

The validity of Langmuir adsorption isotherm was based on very high values of correlation coefficients for the plot of  $C_{inh}/\Theta$  versus  $C_{inh}$  (Figure 4), where the equilibrium constant  $K_{ads}$  is obtained as the reciprocal of intercept. From the values of  $K_{ads}$ , the change in free energy ( $\Delta G_{ads}^{\circ}$ ) is calculated by the relation[10]:

$$\Delta G_{ads}^{\circ} = -RT \ln(K_{ads} \times 55.5) \quad (16)$$

where R is the gas constant and T is the temperature in Kelvin. The value 55.5 is the concentration of water in solution expressed in mol/L.

The adsorption parameters are summarized in Table 4. Generally, when the values of  $\Delta G_{ads}^{\circ}$  approach  $-20 \text{ kJ mol}^{-1}$  or lower, a physisorption is expected[10], but negative values more than  $-40 \text{ kJ mol}^{-1}$  refer to chemisorption and this is associated with a formation of a coordinate type of bond[10]. The value of  $\Delta G_{ads}^{\circ}$  in the present study suggests that the adsorption of molecules of 9-Hydroxyrisperidone may involve both physical and chemical interactions.

**Table 4.** Adsorption parameters of 9-Hydroxyrisperidone adsorbed on steel electrode in 1 M HCl.

| Inhibitor  | Slope | $K_{ads} (M^{-1})$ | $R^2$  | $\Delta G_{ads}^{\circ}$<br>(kJ/mol) |
|------------|-------|--------------------|--------|--------------------------------------|
| <b>HRD</b> | 1.05  | 35665              | 0.9999 | -36.5                                |

### 3.5. Surface characterization

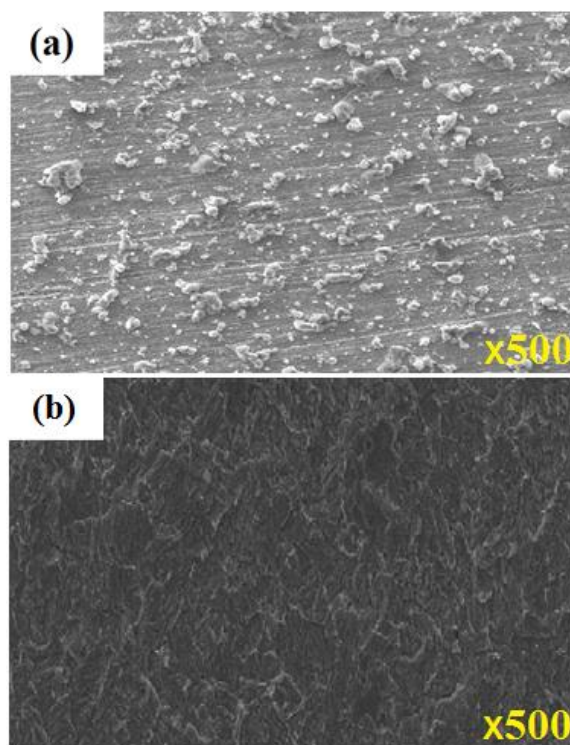


**Figure 6.** SEM images of mild steel: (a) in 1M HCl, (b) in 1M HCl +  $5 \times 10^{-3}$  M of 9-Hydroxyrisperidone after 6h of immersion time.

SEM micrographs of the mild steel have been carried out without and with  $5 \times 10^{-3}$  M of 9-Hydroxyrisperidone. Fig. 6a represents the SEM image of the uninhibited metallic specimen which is drastically damaged and corroded due to free acid attack in the absence of 9-Hydroxyrisperidone. However, in the presence of 9-Hydroxyrisperidone at  $5 \times 10^{-3}$  M, the surface morphology of the metallic specimen (Fig. 6b) was remarkably improved, due to the formation of the protective film by 9-Hydroxyrisperidone molecule on the metallic surface.

### 3.6. DFT calculations

#### 3.6.1. Global reactivity descriptors:

The interaction of corrosion inhibitors and metal surfaces depend on the molecular properties of the inhibitor. These molecular properties include the geometry of the molecule, the electronic properties such as partial atomic charges, frontier molecular orbitals, electronegativity and electronic energy[41,42]. These molecular properties are associated with the presence of particular groups on organic molecules, including the presence of heteroatoms, it bond, aromatic systems and electron density[43,44].

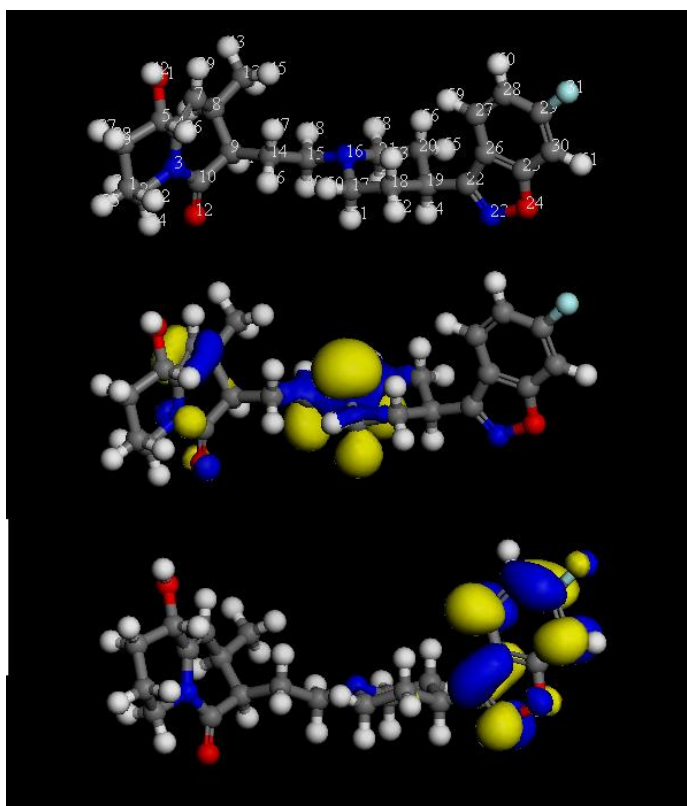


**Figure 7.** (Top) The optimized structure, (center) HOMO and (bottom) LUMO distribution for 9-Hydroxyrisperidone.

It is reported that the molecules with these functional group have high tendency to act as corrosion inhibitors[43]. Quantum chemical calculation was used to elucidate the corrosion inhibition mechanism in terms of electronic and molecular structure properties. Theoretical calculations in the present study were performed using DMol<sup>3</sup> method. The optimized molecular structure obtained from the calculations is given in Figure 7. The HOMO and LUMO orbitals (Figure 7) play a crucial role in the reactivity of inhibitors with the metal surface. The less negative the  $E_{\text{HOMO}}$  of 9-Hydroxyrisperidone molecule the greater its tendency to donate electrons to an electron acceptor such as metals with unfilled d-orbitals[8]. Further, the LUMO energy ( $E_{\text{LUMO}}$ ) indicates the potency of 9-Hydroxyrisperidone molecule to accept electrons; the more negative the value of  $E_{\text{LUMO}}$ , the more probable the 9-Hydroxyrisperidone molecule is to accept electrons[8]. Therefore, the greater the value of  $E_{\text{HOMO}}$  and lower the value of  $E_{\text{LUMO}}$ , the more the capability of 9-Hydroxyrisperidone molecule to adsorb on metal surface which in turn gives rise to better corrosion inhibition efficiency. Similar relationships were reported between the inhibition efficiency and the energy gap ( $\Delta E$ ) in the frontier molecular orbitals (FMOs) ( $\Delta E = E_{\text{LUMO}} - E_{\text{HOMO}}$ )[8]. Some of the most interesting quantities to consider are the location of the HOMO and LUMO orbitals for the inhibitor molecule. In the current study, the HOMO and LUMO orbitals are largely distributed in the heteroatoms and the  $\pi$ -bonds meaning that these regions are the most reactive sites.

The quantum chemical calculations parameters such as;  $E_{\text{HOMO}}$ ,  $E_{\text{LUMO}}$ ,  $\Delta E$  and  $\Delta N$  are represented in Table 5. The HOMO energy ( $E_{\text{HOMO}}$ ) is a measure of a molecule's ability to give electron to an acceptor, while the LUMO energy ( $E_{\text{LUMO}}$ ) is a measure of a molecule's proclivity to receive electron from donor species[8]. The higher the  $E_{\text{HOMO}}$  the better the tendency of electron donation by a molecule and vice versa[8]. Lower  $E_{\text{LUMO}}$  suggests better propensity of a molecule to receive electron and vice versa. Therefore, higher  $E_{\text{HOMO}}$  and/or lower  $E_{\text{LUMO}}$  favor(s) higher corrosion inhibition strength[8]. The smaller value of  $\Delta E$ , the greater the reactivity of a molecule[45]. High reactivity means that the molecule has a greater chance to interact with the metal surface.  $\Delta N$  value, on the other hand, indicates the ability of tested inhibitor to transfer its electrons to metal if  $\Delta N > 0$  and vice versa if  $\Delta N < 0$  [46,47]. According to this criterion, it is obvious from results in Table 5 that 9-Hydroxyrisperidone has higher tendency to donate electrons to a metal surface.

**Table 5.** The quantum chemical parameters of 9-Hydroxyrisperidone at the DFT method.

| Inhibitor | $E_{\text{HOMO}}$<br>(eV) | $E_{\text{LUMO}}$<br>(eV) | $\Delta E_{\text{gap}}$<br>(eV) | $\Delta N_{110}$ |
|-----------|---------------------------|---------------------------|---------------------------------|------------------|
| HRD       | -4.849                    | -1.693                    | 3.156                           | 0.490            |

### 3.6.2. Fukui indices:

In order to gain better insights into the adsorption sites of 9-Hydroxyrisperidone and to support the experimental results, Fukui function analysis was done [48]. They are very useful to evaluate the

most active sites for nucleophilic and electrophilic attacks[48]. Table 6 reports the estimated condensed Fukui indices for 9-Hydroxyrisperidone compound.

The preferred site for nucleophilic attack (shown by the highest value of  $f_k^+$ ) is on N (23), C (27) and C (30) while the highest values of  $f_k^-$  are on C (7), O (12) and N (16). The results obtained from these regions are in agreement with analysis from LUMO and HOMO orbitals because the same predictions from the site with most electron deficient. The results obtained for these regions in nucleophilic and electrophilic attacks support the high capability of tested compound to react with surface of metal through donor-acceptor interactions between most reactive sites of our inhibitor and mild steel surface.

**Table 6.** The Fukui indices of 9-Hydroxyrisperidone calculated using DMol<sup>3</sup> method.

| Atom    | $f_k^+$      | $f_k^-$      | Atom    | $f_k^+$      | $f_k^-$ |
|---------|--------------|--------------|---------|--------------|---------|
| C ( 1)  | -0.001       | -0.011       | C ( 26) | 0.016        | -0.001  |
| C ( 2)  | -0.003       | -0.023       | C ( 27) | <b>0.109</b> | -0.005  |
| N ( 3)  | 0.001        | 0.039        | C ( 28) | 0.024        | 0.007   |
| C ( 4)  | 0.002        | 0.035        | C ( 29) | 0.062        | 0.007   |
| C ( 5)  | 0.000        | -0.005       | C ( 30) | <b>0.094</b> | 0.009   |
| C ( 6)  | -0.001       | -0.012       | F ( 31) | 0.060        | 0.012   |
| C ( 7)  | -0.004       | <b>0.062</b> |         |              |         |
| C ( 8)  | -0.001       | -0.021       |         |              |         |
| C ( 9)  | -0.003       | -0.016       |         |              |         |
| C ( 10) | -0.001       | 0.014        |         |              |         |
| O ( 11) | 0.001        | 0.004        |         |              |         |
| O ( 12) | 0.005        | <b>0.070</b> |         |              |         |
| C ( 13) | -0.001       | -0.012       |         |              |         |
| C ( 14) | -0.004       | -0.018       |         |              |         |
| C ( 15) | -0.013       | -0.023       |         |              |         |
| N ( 16) | -0.004       | <b>0.103</b> |         |              |         |
| C ( 17) | -0.003       | -0.031       |         |              |         |
| C ( 18) | -0.011       | -0.012       |         |              |         |
| C ( 19) | -0.023       | -0.005       |         |              |         |
| C ( 20) | -0.013       | -0.011       |         |              |         |
| C ( 21) | -0.004       | -0.033       |         |              |         |
| C ( 22) | 0.076        | -0.011       |         |              |         |
| N ( 23) | <b>0.123</b> | 0.010        |         |              |         |
| O ( 24) | 0.048        | 0.014        |         |              |         |
| C ( 25) | 0.016        | 0.002        |         |              |         |

### 3.7. Molecular Dynamic (MD) simulations

The electronic properties derived from the calculations of quantum chemistry by the DFT theory are necessary for the understanding of the mechanism of inhibitors but are not sufficient to

describe the metal-molecule interaction[49,50]. In this case, molecular dynamic simulations were largely used to investigate the inhibition action of chemical species used as inhibitors. The binding and interaction energies of the adsorbed inhibitors have been approximated when the simulation system reached their equilibrium state[7]. The best adsorption configuration of the studied molecules on Fe (110) surface is shown in Figure 8 while the interaction and binding energies are placed in Table 7. Otherwise, it can be seen from the data in Table 7 that the binding energy of the adsorption of inhibitor on Fe (110) surface is very high and positive suggesting the high stability of the adsorbed inhibitor[7,10]. The higher negative values of interaction energy can be attributed to the strong adsorption of 9-Hydroxyrisperidone molecules on the Fe surface[7,10]. These results are in good agreement with experimental studies which have shown that tested drug acts as good corrosion inhibitor of mild steel.

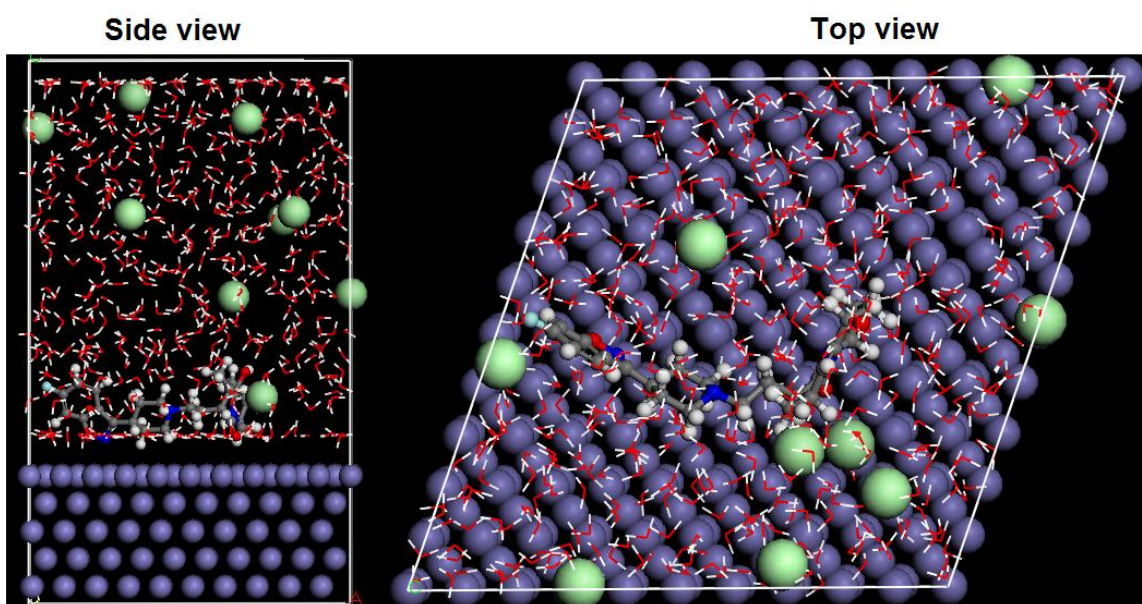


**Figure 8.** Side and top views of the final adsorption of 9-Hydroxyrisperidone on the iron surface.

**Table 7.** Interaction and binding energies obtained from MD simulations for the most stable configurations adsorption of 9-Hydroxyrisperidone on iron surface

| System  | $E_{\text{Interaction}}$<br>(kJ/mol) | $E_{\text{Binding}}$<br>(kJ/mol) |
|---|--------------------------------------|----------------------------------|
| Fe + <b>HRD</b> /491H <sub>2</sub> O, 9Cl <sup>-</sup> and 9H <sub>3</sub> O <sup>+</sup> | -784,63                              | 784,63                           |

#### 4. CONCLUSION

In summary, 9-Hydroxyrisperidone was used as corrosion inhibitor for mild steel in 1.0 M HCl. The study was carried out using several methods which include weight loss, electrochemical analysis, SEM and computational calculations. 9-Hydroxyrisperidone shows a good inhibition performance. The

study reveals that 9-Hydroxyrisperidone suppresses both the anodic and cathodic process (mixed-typed inhibitor) following Langmuir adsorption model. SEM and AFM analyses revealed that 9-Hydroxyrisperidone protects the surface of mild steel in the tested acid. The experimental results were very well supported by quantum chemical calculations and MD simulations.

#### ACKNOWLEDGEMENTS

The authors extend their appreciation to the Deanship of Scientific Research at King Khalid University for funding this work through research groups program under grant number R.G.P-21-38

#### Reference

1. K.K. Anupama, K. Ramya and A. Joseph, *J. Mol. Liq.*, 216 (2016) 146.
2. C. Verma, M. Quraishi, E. Ebenso, I. Obot and A. El Assyry, *J. Mol. Liq.*, 219 (2016) 647.
3. C. Verma, L.O. Olasunkanmi, I.B. Obot, E.E. Ebenso and M.A. Quraishi, *RSC Adv.*, 6 (2016) 15639.
4. R. Salghi, S. Jodeh, E.E. Ebenso, H. Lgaz, D. Ben Hmamou, I.H. Ali, M. Messali, B. Hammouti and N. Benchat, *Int. J. Electrochem. Sci.*, 12 (2017) 3309.
5. T. Laabaissi, H. Lgaz, H. Oudda, F. Benhiba, H. Zarrok, A. Zarrouk, A. El Midaoui, B. Lakhrissi and R. Tourir, *J. Mater. Environ. Sci.*, 8 (2017) 1054.
6. Y. El Aoufir, J. Sebhaoui, H. Lgaz, Y. El Bakri, A. Zarrouk, F. Bentiss, A. Guenbour, E.M. Essassi and H. Oudda, *J. Mater. Environ. Sci.*, 8 (2017) 2161.
7. H. Lgaz, R. Salghi, S. Jodeh and B. Hammouti, *J. Mol. Liq.*, 225 (2017) 271.
8. M. Messali, H. Lgaz, R. Dassanayake, R. Salghi, S. Jodeh, N. Abidi and O. Hamed, *J. Mol. Struct.*, 1145 (2017) 43.
9. R. Salghi, S. Jodeh, E.E. Ebenso, H. Lgaz, D. Ben Hmamou, M. Belkhaouda, I.H. Ali, M. Messali, B. Hammouti and S. Fattouch, *Int. J. Electrochem. Sci.*, 12 (2017) 3283.
10. H. Lgaz, K. Subrahmanya Bhat, R. Salghi, Shubhalaxmi, S. Jodeh, M. Algarra, B. Hammouti, I.H. Ali and A. Essamri, *J. Mol. Liq.*, 238 (2017) 71.
11. Y. Abboud, A. Abourriche, T. Ainane, M. Charrouf, A. Bennamara, O. Tanane and B. Hammouti, *Chem. Eng. Commun.*, 196 (2009) 788.
12. M. Abdallah, *Corros. Sci.*, 46 (2004) 1981.
13. K. Anuradha, R. Vimala, B. Narayanasamy, J.A. Selvi and S. Rajendran, *Chem. Eng. Commun.*, 195 (2007) 352.
14. N.O. Eddy, U.J. Ibok, P.O. Ameh, N.O. Alobi and M.M. Sambo, *Chem. Eng. Commun.*, 201 (2014) 1360.
15. E.E. Oguzie, C.O. Akalezi, C.K. Enenebeaku and J.N. Aneke, *Chem. Eng. Commun.*, 198 (2010) 46.
16. B. Delley, *J. Chem. Phys.*, 92 (1990) 508.
17. B. Delley, *J. Chem. Phys.*, 113 (2000) 7756.
18. Materials Studio, Revision 6.0, Accelrys Inc., San Diego, USA, 2013.
19. R.S. Mulliken, I, *J. Chem. Phys.*, 23 (1955) 1833.
20. M.J. Dewar and W. Thiel, *J. Am. Chem. Soc.*, 99 (1977) 4899.
21. R.G. Pearson, *Coord. Chem. Rev.*, 100 (1990) 403.
22. S. Martinez, *Mater. Chem. Phys.*, 77 (2003) 97.
23. R.G. Pearson, *J. Org. Chem.*, 54 (1989) 1423.
24. R.G. Pearson, *Inorg. Chem.*, 27 (1988) 734.
25. R.G. Pearson, *Coord. Chem. Rev.*, 100 (1990) 403.
26. A. Kokalj, *Chem. Phys.*, 393 (2012) 1.

27. R.G. Parr and W. Yang, *J. Am. Chem. Soc.*, 106 (1984) 4049.
28. R.R. Contreras, P. Fuentealba, M. Galván and P. Pérez, *Chem. Phys. Lett.*, 304 (1999) 405.
29. S.W. Bunte and H. Sun, *J. Phys. Chem. B.*, 104 (2000) 2477.
30. Z. Zhang, N.C. Tian, X.D. Huang, W. Shang and L. Wu, *RSC Adv.*, 6 (2016) 22250.
31. L. Afia, O. Hamed, M. Larouj, H. Lgaz, S. Jodeh, R. Salghi, (2017) in press, doi:10.1007/s12666-017-1094-x.
32. Y. El Aoufir, Y. El Bakri, H. Lgaz, A. Zarrouk, R. Salghi, I. Warad, Y. Ramli, A. Guenbour, E.M. Essassi and H. Oudda, *J. Mater. Environ. Sci.*, 8 (2017) 3290.
33. B. El Makrini, H. Lgaz, K. Toumiat, R. Salghi, S. Jodeh, G. Hanbali, M. Belkhaouda and M. Zougagh, *J. Pharm. Biol. Chem. Sci.*, 7 (2016) 2277.
34. L. Adardour, H. Lgaz, R. Salghi, M. Larouj, S. Jodeh, M. Zougagh, O. Hamed and H. Oudda, *Pharm. Lett.*, 8 (2016) 212.
35. H. Lgaz, M. Saadouni, R. Salghi, S. Jodeh, Y. Ramli, A. Souizi and H. Oudda, *Pharm. Lett.*, 8 (2016) 167.
36. M. Saadouni, M. Larouj, R. Salghi, H. Lgaz, S. Jodeh, M. Zougagh and A. Souizi, *Pharm. Lett.*, 8 (2016) 65.
37. L. Adardour, H. Lgaz, R. Salghi, M. Larouj, S. Jodeh, M. Zougagh, O. Hamed and M. Taleb, *Pharm. Lett.*, 8 (2016) 173.
38. L.O. Olasunkanmi, I.B. Obot and E.E. Ebenso, *RSC Adv.*, 6 (2016) 86782.
39. M. Gholami, I. Danaee, M.H. Maddahy and M. RashvandAvei, *Ind. Eng. Chem. Res.*, 52 (2013) 14875.
40. X. Gao, S. Liu, H. Lu, F. Gao and H. Ma, *Ind. Eng. Chem. Res.*, 54 (2015) 1941.
41. R.N. Singh, A. Kumar, R.K. Tiwari and P. Rawat, *Spectrochim. Acta. A. Mol. Biomol. Spectrosc.*, 112 (2013) 182.
42. H. Jafari, I. Danaee, H. Eskandari and M. RashvandAvei, *J. Mater. Sci. Technol.*, 30 (2014) 239.
43. L.M. Rodríguez-Valdez, W. Villamizar, M. Casales, J.G. González-Rodríguez, A. Martínez-Villafañe, L. Martinez and D. Glossman-Mitnik, *Corros. Sci.*, 48 (2006) 4053.
44. D. Daoud, T. Douadi, H. Hamani, S. Chafaa and M. Al-Noaimi, *Corros. Sci.*, 94 (2015) 21.
45. N.A. Wazzan, *J. Ind. Eng. Chem.*, 26 (2015) 291.
46. A. Kokalj, *Electrochimica Acta*, 56 (2010) 745.
47. N. Kovačević and A. Kokalj, *Corros. Sci.*, 53 (2011) 909.
48. H. Lgaz, O. Benali, R. Salghi, S. Jodeh, M. Larouj, O. Hamed, M. Messali, S. Samhan, M. Zougagh and H. Oudda, *Pharma Chem.*, 8 (2016) 172.
49. Z. Zhang, N. Tian, X. Huang, W. Shang and L. Wu, *RSC Adv.*, 6 (2016) 22250.
50. S.-W. Xie, Z. Liu, G.-C. Han, W. Li, J. Liu and Z. Chen, *Comput. Theor. Chem.*, 1063 (2015) 50.